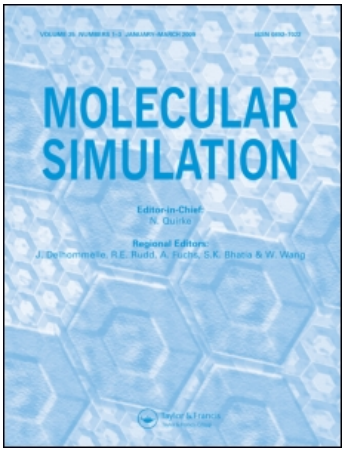

Molecular Simulation
Publication details, including instructions for authors and subscription information:
http://www.informaworld.com/smpp/title~content=t713644482

Calculation of the effect of intrinsic point defects and volume swelling in the nuclear magnetic resonance spectra of $ZrSiO_4$

J. M. Pruneda[a]; L. Le Polles[a]; I. Farnan[a]; K. Trachenko[a]; M. T. Dove[a]; E. Artacho[a]
[a] Department of Earth Sciences, University of Cambridge, Cambridge, UK

To cite this Article Pruneda, J. M. , Polles, L. Le , Farnan, I. , Trachenko, K. , Dove, M. T. and Artacho, E.(2005) 'Calculation of the effect of intrinsic point defects and volume swelling in the nuclear magnetic resonance spectra of $ZrSiO_4$', Molecular Simulation, 31: 5, 349 — 354
To link to this Article: DOI: 10.1080/08927020500066916
URL: http://dx.doi.org/10.1080/08927020500066916

Molecular Simulation, Vol. 31, No. 5, April 2005, 349–354

Taylor & Francis
Taylor & Francis Group

Calculation of the effect of intrinsic point defects and volume swelling in the nuclear magnetic resonance spectra of $ZrSiO_4$

J. M. PRUNEDA*, L. LE POLLES†, I. FARNAN, K. TRACHENKO, M. T. DOVE and E. ARTACHO

Department of Earth Sciences, University of Cambridge, Downing Street, Cambridge CB2 3EQ, UK

(Received July 2004; in final form September 2004)

A variety of computational tools have been used to study the chemical properties of point defects in the crystalline phase of $ZrSiO_4$, and their effect in its lattice parameters. The experimental evidence of a large anisotropic volume swelling in natural and artificially irradiated samples of $ZrSiO_4$ was used to select the subset of defects that give similar lattice swelling for the concentrations studied, namely interstitials of O and Si, and the anti-site Zr_{Si}. Using the relaxed atomic structures, the nuclear magnetic resonance spectra were calculated by means of first principles density functional methods, in order to find additional evidence for the presence of high concentrations of some of these defects in irradiated zircon. The results obtained for the defects singled out before are still compatible with available experimental information. Our calculations also show that volume swelling in crystalline $ZrSiO_4$ would produce a considerable displacement of the ^{17}O and ^{91}Zr chemical shifts towards higher values, whereas the ^{29}Si spectra would be largely independent of the defect-induced swelling.

Keywords: Crystalline phase of $ZrSiO_4$; Nuclear magnetic resonance; Amorphization; Anisotropic; Awelling; Point defects

1. Introduction

The ability to accomodate actinides, its high resistance to corrosion and low thermal conductivity makes zircon a candidate ceramic for immobilization of nuclear waste [1,2]. Defect accumulation and its consequences for the degradation of the mechanical properties have to be understood in order to control possible leaching, creep and fatigue of these materials [3]. Large concentrations of irradiation induced defects produce strains that affect the crystalline lattice structure, which can undergo amorphization, change into a different crystalline phase, or remain in the same crystal phase with changes in the lattice parameters. In addition to these changes, the electronic properties are affected in a way that can produce substantial differences in the physical and chemical properties of the original material.

After a radioactive impurity undergoes an α-decay transition, heavy damage is produced in the crystalline structure. When the dose of α-decays is not too large there is a coexistence between the amorphized (metamict) region and the crystalline phase, the latter containing point defects. X-ray experiments on damaged samples show a unit cell volume expansion of up to 5% in the crystalline phase. This volume swelling is anisotropic in natural samples, giving an increase of up to $\sim$1.5% along the *ab*-plane, and $\sim$2.0% along the *c*-axis [4–6]. For Pu-doped samples, the swelling is much less anisotropic, suggesting a preferential relaxation of the expansion along the *a*-axis over geological times in the natural samples. ^{29}Si nuclear magnetic resonance (NMR) studies of damaged zircon indicate changes in the Si local environment towards a polimerization of the structure during amorphization [7]. This means that Si—O—Si bonds are formed in the amorphous region and the initially isolated SiO_4 tetrahedra are connected through an oxygen bridge. This polymerization requires that on average the number of oxygens per Si is smaller in the amorphized region, possibly favouring the presence of interstitial oxygens in the rest of the system.

Theoretical studies of neutral point defects show that the oxygen interstitial is the most stable, followed by cation antisite defects [8,9]. In previous work [10], we used first principles electronic structure calculations to study the influence of very high concentrations of neutral and charged point defects on the crystalline

*Corresponding author. E-mail: mpru02@esc.cam.ac.uk
†Present address: Ecole Nationale Supérieure de Chimie de Rennes, Laboratoire CSIM—UMR 6511, Institut de Chimie the Rennes, Campus de Beaulieu, 35700 Rennes, France.

Molecular Simulation
ISSN 0892-7022 print/ISSN 1029-0435 online © 2005 Taylor & Francis Group Ltd
http://www.tandf.co.uk/journals
DOI: 10.1080/08927020500066916

structure of zircon, showing that interstitials of O and Si, and the antisite defect with Zr in the Si site, can give lattice expansions similar to the ones experimentally observed. We now perform first principles calculations to obtain the NMR spectra produced by the arrangement of atoms close to these point defects, which could provide further evidence for their presence in the crystalline phase of irradiated zircons. In both works, the use of different computational codes and platforms, and the parallel calculations of the many defect candidates considered, was facilitated by the Condor distributed computing system [11] and implemented as part of the *e*Minerals minigrid [12,13].

2. Methodology

Experimentally, the change in the lattice parameters can be directly monitored using X-ray diffraction. Point defects would be randomly distributed through the crystal lattice. If the number of accumulated α-decays is not too large ($\sim 2 \times 10^{18}$ α/g), and we assume that $\sim$220 atoms are displaced by each α particle [5], we can expect concentrations of 2×10^{21} defects/cm^3. That is roughly one defect for each two unit cells, the kind of concentration considered in this work.

Available experiments are not able to suggest a limited range of defects. Hence, we used a combinatorial approach similar to the one described in [14]. We considered a catalogue of neutral and charged intrinsic defects, that includes interstitials (X_i) and vacancies (V_X) of the three elements (X) present in zircon, Zr and Si antisite defects (Zr_{Si} and Si_{Zr}), Frenkel pairs (X_{FP}), and other combinations of interstitials and vacancies. The theoretical characterization of the relevant point defects was performed with a combination of computational methods for different architectures.

The structures of point defects were calculated with the self-consistent *ab initio* siesta method [15,16], using density functional theory (DFT) [17,18] within the local density approximation (LDA) [19]. An heterogeneous set of PCs under the *Condor* management system [20] was used. The host crystal ($ZrSiO_4$, space group $I4_1/amd$) is represented by a supercell generated by repetition of the conventional tetragonal unit cell (4 formula units). A point defect is then introduced inside a supercell (adding atoms for interstitials, removing atoms for vacancies, etc) that is a $n \times m \times p$ repetition of the tetragonal unit cell along the three principal axes. We considered cells with 24, 48 and 96 atoms, corresponding to $1 \times 1 \times 1$, $1 \times 1 \times 2$ and $2 \times 2 \times 1$. The minimum-energy structure for each defect was obtained by relaxing with a conjugate-gradient minimization for the forces and stresses. The lattice vectors and the atomic positions were allowed to relax until atomic forces and stresses from the electronic structure calculations were smaller than 30 meV/Å and 6 meV/Å^3, respectively.

The NMR chemical shifts were obtained for the relaxed $1 \times 1 \times 1$ structures of siesta, by calculating the shielding of the nuclei due to the electronic current induced by an external magnetic field. This technique[21] is computationally very demanding and the use of high-performance computer facilities is required. We used the paratec code, [22] which has already been applied to study the effects of radiation damage in zircon[23] The chemical shifts of ^{29}Si and ^{17}O in quartz [24] (SiO_2) and zirconia [25] (ZrO_2) are used as a reference to fix the scale to experiments. For ^{91}Zr we studied only shifts relative to the theoretically obtained crystalline signal.

3. Results

The effect of point defects in the lattice structure after relaxation is summarized in figure 1, where we show the changes in volume, and the anisotropy ($\Delta a/\Delta c$) relative to the neutral structure for the defects studied. In general, there is a considerable anisotropy in the relaxation, with different changes in the *c*-axis and in the *ab*-plane. Experimentally [4], an increase in *c* of $\sim$2% is observed, while *a* increases by a smaller amount ($\sim$1.5%). From this catalogue, we extract a subset of defects that produce a swelling of the lattice that is compatible with the experimental observations (see figure 1). Firstly, a positive volume expansion (as big as 5%) is expected. Secondly, $\Delta a/\Delta c$ has to be positive and smaller than 1 (larger expansion in *c* than in *a*). These requirements give O_i, Si_i and Zr_{Si} (structures in figure 2) as possible originators of the swelling. A detailed description of the catalogue is described in [10].

The calculated NMR chemical shifts for ^{17}O and ^{29}Si in each of the atomic positions of the cell used to simulate the defects, are shown in tables 1 and 2. Table 3 shows the chemical shifts for ^{91}Zr relative to the value obtained for crystalline $ZrSiO_4$. Due to the high concentration of point defects, there are considerable distortions in the atomic structure that are revealed in the chemical shifts. In the following we will present a detailed description of the defects' spectra.

3.1 Oxygen interstitial

The interstitial oxygen (O_1 in figure 2) forms a dumb-bell structure with an oxygen atom (O_{20}) in the crystalline structure. The high ionicity of the crystal forces the interstitial to a position where the electronic density screens the coulomb interactions. The covalent bond to the interstitial oxygen reduces the strength of the Si_8—O_{20} bond, and the SiO_4 tetrahedra loses part of its charge. Mulliken population analysis shows that the charges in the interstitial and in the lattice oxygen are similar, and slightly smaller (6%) than in other oxygen atoms. This also affects the ^{29}Si chemical shifts of the tetrahedral silicon, to which O_{20} was originally bonded, that is displaced towards more negative values

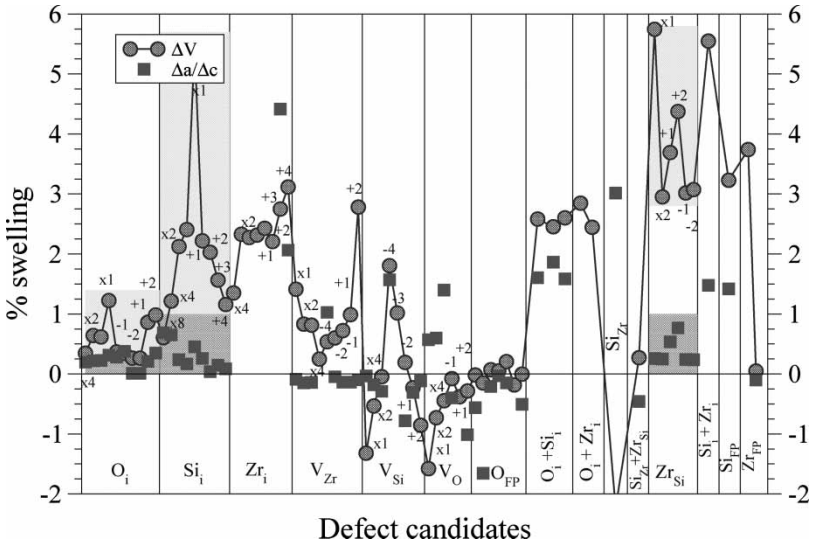

Figure 1. Lattice volume % swelling (circles) and anisotropic factor $\Delta a/\Delta c$ (squares) for the set of defects considered in this work. X_i, V_X, X_{FP} denote interstitials, vacancies and Frenkel pairs of X, respectively. The different charge states are denoted by $\pm q$ and the different concentrations of defects by $\times n$, with n denoting the number of repetitions of the tetragonal unit cell (cells with 24, 48 and 96 atoms, for $n = 1, 2, 4$ respectively). Unless stated, the neutral defect with $n = 2$ cell is considered.

(-112 ppm), on the edge of what is observed in the damaged samples [7], as seen in the figure 4. This rises interesting questions on the concentration of interstitials of oxygen in the samples, e.g. whether or not strain fields can spread the peak and shift it to higher value, thus allowing for the expected high concentration of O_i. Answering this is, beyond the scope of this work. For the interstitial oxygen, we obtained a ^{17}O shift much higher than for crystalline oxygen (282 ppm). Also the chemical shift for ^{91}Zr changes towards lower values, except for the one closest to the interstitial oxygen (Zr_3), which displays a larger value.

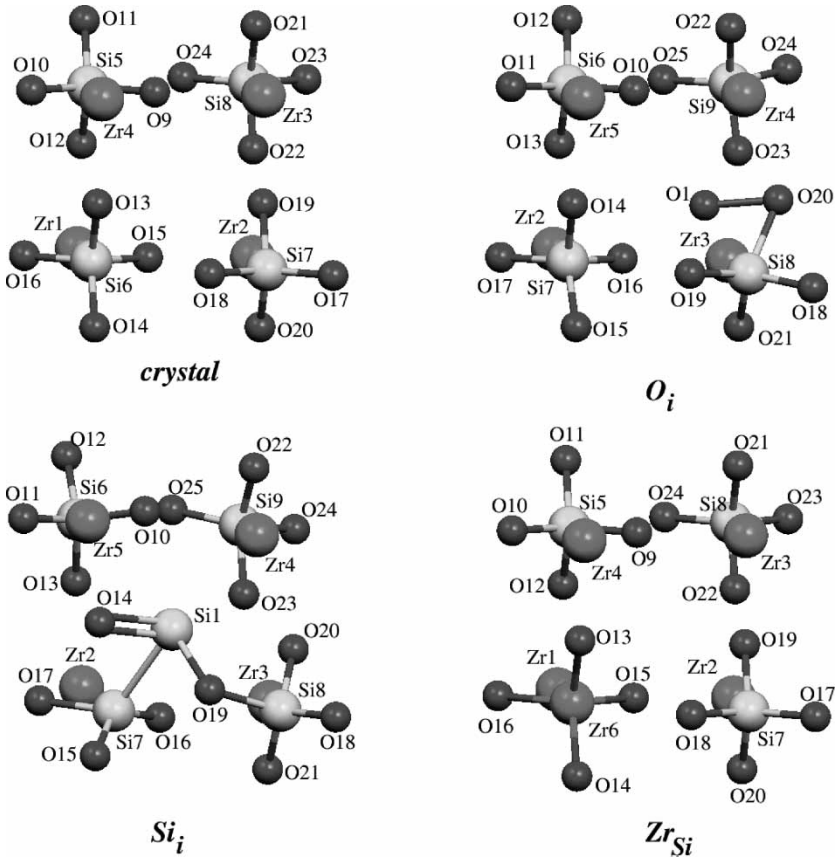

Figure 2. Atomic structures for the crystalline $ZrSiO_4$, and O_i, Si_i and Zr_{Si} point defects in the $1 \times 1 \times 1$ cell.

Table 1. Calculated δ ^{17}O chemical shifts (in ppm) for the three point defects considered. The atomic labels correspond to figure 2. For the crystalline structure, we obtained 170.1 ppm, in excellent agreement with the ~170 ppm observed [24].

	O_i	Si_i	Zr_{Si}
O1	282		
O9			148
O10	196	117	148
O11	154	167	158
O12	199	224	158
O13	158	149	464
O14	164	244	464
O15	162	201	464
O16	169	322	464
O17	168	212	158
O18	183	178	158
O19	165	95	148
O20	178	203	148
O21	177	172	166
O22	176	161	166
O23	144	166	166
O24	166	188	166
O25	169	114	

3.2 Silicon interstitial

In this case, the interstitial (Si_1) does not form clear bonds with the neighbouring atoms [10] (the connections between Si_1, Si_7, O_{14} and O_{19} in figure 2 are artificial and were used as a reference for the position of the interstitial relative to the other atoms), but the lattice is strongly distorted and the SiO_4 and ZrO_8 polyhedra change to accommodate to the presence of the interstitial. Upon removal of electrons from Si_i, new atomic structures are obtained, with the interstitial causing oxygen atoms to approach, and neutralize the charge around it. The coordination of Si_i^{+n} increases with n and this can give a polimerization of the structure and a change of the chemical shifts of crystalline Si. The interstitial Si has a higher value of δ (less negative) than the tetrahedrally coordinated silicons, that also have increased shifts relative to the crystalline structure. The strong dispersion in the ^{17}O shifts is a consequence of the large distortion of the cell. No clear trend emerges from the shifts, with displacements to higher values (322 ppm for the O_{16}) as well as to lower values (95 ppm for O_{19}). For ^{91}Zr the shifts decrease considerably, a consequence again of the distortion of the polyhedra.

Table 2. Calculated δ ^{29}Si chemical shifts (in ppm) for the three point defects considered. The atomic labels correspond to figure 2. The shift obtained in the crystalline structure (−78.6 ppm) compares relatively well with the experimental value of −81.5 ppm [26].

	O_i	Si_i	Zr_{Si}
Si1		−7.5	
Si5			−82
Si6	−84	−76	
Si7	−81	−47	−82
Si8	−112	−75	−81
Si9	−86	−86.6	

Table 3. Calculated δ ^{91}Zr chemical shifts (in ppm) relative to the crystalline $ZrSiO_4$, for the three point defects considered. The atomic labels correspond to figure 2.

	O_i	Si_I	Zr_{Si}
Zr1	−24		49
Zr2	−38	−54	−39
Zr3	65	−180	−65
Zr4	−30	−404	−39
Zr5		−121	
Zr6			−432

3.3 Cation antisite Zr_{Si}

In Zr_{Si}, the Zr_6 forms a tetrahedron with four oxygen around it, with bond lengths of 1.9Å(+17% longer than the Si—O bonds). The Si—O distances increase slightly (~ +1%) close to the defect, due to the increase in the lattice parameters. This explains the low value of the ^{17}O chemical shift. A clear signal would be expected at ~464 ppm related to the oxygens surrounding the Zr_{Si}. The shifts are homogenous for the ^{29}Si signals towards slightly smaller values. For ^{91}Zr, a new peak related to the Zr_{Si} would appear ~432 ppm lower than the crystalline value.

3.4 Dependence of the Chemical Shifts with the Lattice Parameters

The amorphised regions produced by radiation cascades impose a tensile stress on the crystalline matrix that

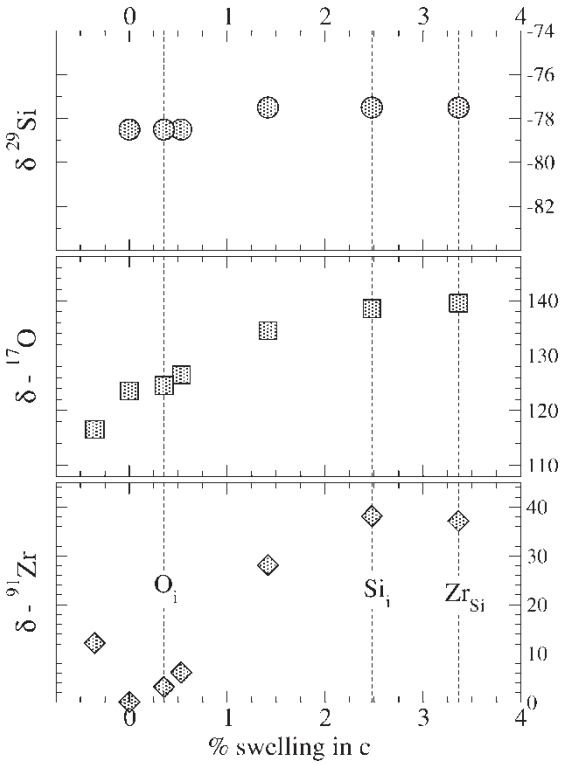

Figure 3. Changes in the ^{17}O and ^{29}Si chemical shifts (in ppm) as a function of the swelling in the c lattice paramater relative to the experimental value. The grid lines correspond to the relaxed parameters for the corresponding point defects at the concentration of one defect for each two unit cells.

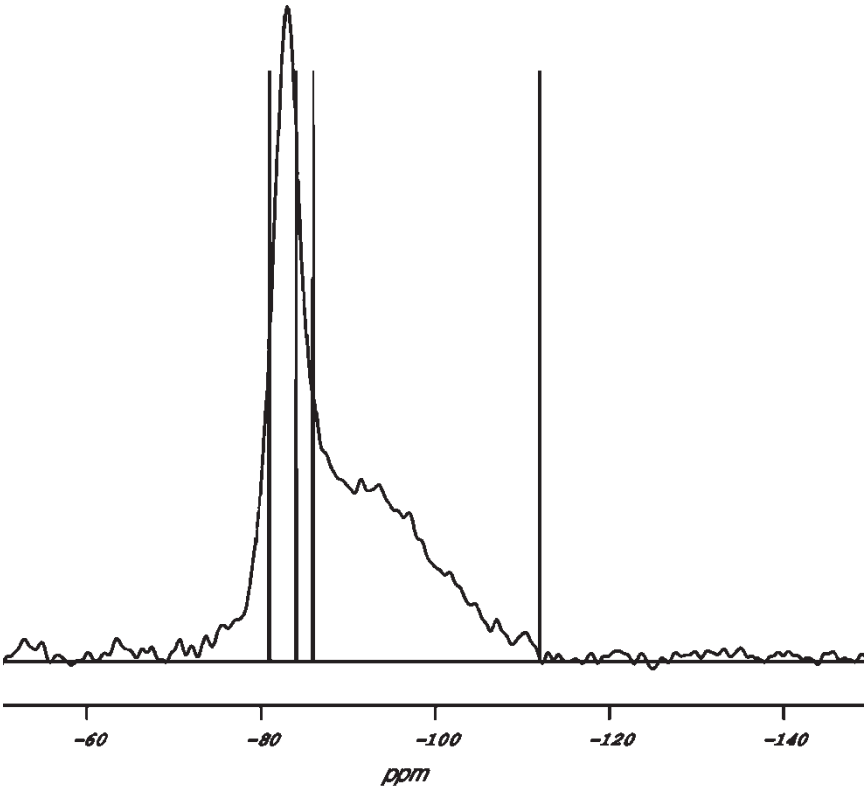

Figure 4. ^{29}Si chemical shifts obtained for O_i point defect, as compared with experimental observation [7], in a sample with an accumulated α dose of 2.9×10^{18} α/g. The line at -112 ppm corresponds to the Si atom that is closer to the interstitial's dumb-bell.

contributes to the expansion of the unit cell induced by point defects [27]. In addition to this elastic swelling observed by X-ray experiments, there is a large inelastic swelling of up to 20% that is shown in the changes of the density of the samples. It is thought that this inelastic expansion might come from the overlap of cascades [28]. It is interesting to see the dependence of the chemical shifts of crystalline bulk zircon with the swelling induced by the radiation damage, independently of the origin of that swelling (point defect, amorphous domains or overlap of damaged regions). For that, we performed calculations of the perfect crystalline structure with different values of the lattice parameters (keeping the internal atomic parameters u and v fixed). In figure 3 we show a plot of δ, for ^{29}Si, ^{17}O and ^{91}Zr, as a function of the swelling in the c lattice parameter. It is clear that, though the ^{29}Si shift seems to be quite, independent, of the lattice expansion, there is a clear dependence for the ^{17}O and ^{91}Zr on c, that saturates for a swelling of $\sim 3\%$. Changes in c similar to the ones observed for irradiated samples can give shifts of tens of ppm in the chemical shifts, just coming from the swelling of the crystalline phase.

4. Conclusions

Simulations of high concentration of point defects in $ZrSiO_4$ have been performed to study the effect of these on the lattice swelling under radiation damage. Based on experimental evidence of anisotropic swelling, we have selected a set of defects as good candidates to be responsible for the lattice expansion in crystalline zircon, and performed NMR calculations searching for experimental traces of these defects in samples with low radiation dose. The results show that O_i and Zr_i should give a clear signal in the ^{17}O NMR spectra close to 280 and 460 ppm. The oxygen interstitial also distorts the chemical environment close to a silicon atom, inducing a shift of the ^{29}Si signal towards lower values (more negative), but the strain fields across the sample may affect its position and shape. Additional work is required to understand the effect of high concentrations of this defect. We also observed that the volume swelling in irradiated samples would not affect the chemical shift of ^{29}Si, while on the contrary it would produce a displacement towards higher values for the ^{17}O and ^{91}Zr NMR signals.

Acknowledgements

This work was supported by British Nuclear Fuels (BNFL), CMI and NERC (through the eScience project, "Environment from the Molecular Level"). Computational resources were provided by the Cambridge-Cranfield High Performance Computing Facility. Calculations were performed with PARATEC (PARAllel Total Energy Code) by B. Pfrommer, D. Raczkowski, A. Canning, S.G. Louie, Lawrence Berkeley National Laboratory

(with contributions from F. Mauri, M. Cote, Y. Yoon, C. Pickard and P. Haynes) for more information see www.nersc.gov/projects/paratec. We would like to thank E. K. H. Salje, G. Lumpkin, M. Yang, S. Rios, S. A. T. Redfern, K. Whittle, S. E. Ashbrook, E. Maddrell, J. P. Attfield, C. J. Pickard, J. Yates and F. Mauri for helpful discussions on radiation damage, and on calculation of NMR spectra.

References

[1] W.J. Weber, et al. Radiation effects in crystalline ceramics for the immobilization of high-level nuclear waste and plutonium. *J. Mater. Res.*, **13**, 1434 (1998).
[2] R.C. Ewing, W. Lutze, W.J. Weber. Zircon: A host-phase for the disposal of weapons plutonium. *J. Mater. Res.*, **10**, 243 (1995).
[3] K.E. Sickafus, L. Minervini, R.W. Grimes, J.A. Valdez, M. Ishimaru, F. Li, K.J. McClellan. Radiation tolerance of complex oxides. *Science*, **289**, 5479 (2000).
[4] H.D. Holland, D. Gottfried. The effect of nuclear radiation on the structure of zircon. *Acta Cryst.*, **8**, 291 (1955).
[5] S. Ríos, T. Malcherek, E.K.H. Salje, C. Domeneghetti. Localized defects in radiation-damaged zircon. *Acta Cryst.*, **B56**, 947 (2000).
[6] W.J. Weber. Alpha-decay-induced amorphization in complex silicate structures. *J. Am. Ceram. Soc.*, **76**, 1729 (1993).
[7] I. Farnan, E.K.H. Salje. The degree and nature of radiation damage in zircon observed by 29Si nuclear magnetic resonance. *J. Appl. Phys.*, **89**, 2084 (2001).
[8] J.-P. Crocombette. Theoretical study of point defects in crystalline zircon. *Phys. Chem. Miner.*, **27**, 138 (1999).
[9] J.M. Pruneda, E. Artacho. Energetic of intrinsic point defects in $ZrSiO_4$, (submitted).
[10] J.M. Pruneda, T.D. Archer, E. Artacho. Intrinsic point defects and volume swelling in ZrSiO4 under irradiation. *Phys. Rev. B*, (to be published).
[11] D. Thain, T. Tannenbaum, M. Livny M. Condor and the Grid. In *Grid Computing: Making The Global Infrastructure a Reality*, F Berman, AJG Hey, G Fox, Wiley John (Eds.), pp. 11 (2003), Chapter 11.
[12] M. Calleja, L. Blanshard, R. Bruin, C. Chapman, A. Thandavan, R. Tyer, P. Wilson, V. Alexandrov, R.J. Allen, J. Brodholt, M.T. Dove, W. Emmerich, K. Kleese van Dam. Grid tool integration within the eMinerals project. Proceedings of the UK e-Science All Hands Meeting 2004, pp. 812817 (2004), (ISBN 1-904425-21-6).
[13] M. Calleja, R. Bruin, M.G. Tucker, M.T. Dove, R.P. Tyer, L.J. Blanshard, K. Kleese van Dam, R.J. Allan, C. Chapman, W. Emmerich, P.B. Wilson, J.P. Brodholt, A. Thandavan, V.N. Alexandrov. Collaborative grid infrastructure for molecular simulations: The eMinerals minigrid as a prototype integrated compute and data grid. Molecular Simulations, in press (same issue).
[14] C. Chapman, W. Emmerich, J. Wakelin, E. Artacho, M. Dove, R. Bruin. Workflow issues in atomistic simulations. Molecular Simulations, in press (same issue).
[15] P. Ordejón, E. Artacho, J.M. Soler. Self-consistent order-N density-functional calculations for very large systems. *Phys. Rev. B*, **53**, 10441 (1996).
[16] J.M. Soler, E. Artacho, J.D. Gale, A. García, J. Junquera, P. Ordejón, D. Sánchez-Portal. The siesta method for ab initio order-N materials simulation. *J. Phys.: Condens. Mat.*, **14**, 2745 (2002).
[17] P. Hohenberg, W. Kohn. Inhomogeneous electron gas. *Phys. Rev.*, **136**, B864 (1964).
[18] W. Kohn, L.J. Sham. Self-consistent equations including exchange and correlation effects. *Phys. Rev.*, **140**, A1133 (1965).
[19] D.M. Ceperley, B.J. Alder. Ground state of the electron gas by stochastic method. *Phys. Rev. Lett.*, **45**, 566 (1980).
[20] , http://www.cs.wisc.edu/condor
[21] C.J. Pickard, F. Mauri. All-electron magnetic response with pseudopotentials: NMR chemical shifts. *Phys. Rev. B*, **63**, 245101 (2001).
[22] Pfrommer, et al. http://www.nersc.gov.projects/paratec
[23] I. Farnan, E. Balan, C.J. Pickard, F. Mauri. The effect of radiation damage on local structure in crystalline ZrSiO4: Investigating the 29Si NMR response to pressure in zircon and reidite. *Am. Mineral.*, **88**, 1663 (2003).
[24] K.J.D. MacKenzie, M.E. Smith. Multinuclear Solid-State Nuclear Magnetic Resonance of Inor-ganic Materials, Pergamon Press Inc, (2002).
[25] A.V. Chadwick, G. Mountjoy, V.M. Nield, I.J.F. Poplett, M.E. Smith, J.H. Strange, M.G. Tucker. Solid-State NMR and X-ray studies of the structural evolution of nanocrystalline zirconia. *Chem. Mater.*, **13**, 1219 (2001).
[26] M. Magi, E. Lippmaa, A. Samoson, G. Engelhardt, A.R. Grimmer. Solid-State high-resolution Silicon-29 chemical shifts in silicates. *J. Phys. Chem.*, **88**, 1518 (1984).
[27] K. Trachenko, M.T. Dove, E.K.H. Salje. Structural changes in zircon under alpha-decay irradi-ation. *Phys. Rev. B*, **65**, 180102 (2002).
[28] K. Trachenko, M.T. Dove, E.K.H. Salje. Large swelling and percolation in irradiated zircon. *J. Phys.: Condens. Mat.*, **15**, L1 (2003).